Indian J.Sci.Res. 4(1) : 45-52, 2013

ISSN : 0976-2876 (Print)
ISSN : 2250-0138 (Online)

A COMPARATIVE ALGORITHM FOR OFDM BASED ON MULTIPLE CHANNEL SUPPORTED TIMING SYNCHRONIZATION

REZA SHAHBAZIAN[a1] AND BAHMAN ABOLHASSANI[b]

Department of Electrical Engineering, Iran University of Science and Technology, Tehran, Iran
[a]E-mail: shahbazian@elec.iust.ac.ir
[b]E-mail: abolhassani@iust.ac.ir

ABSTRACT

In this paper, a wireless MAN OFDM systems algorithm based on robust timing synchronization has been proposed by us. A combination of FFT based timing and frame synchronization makes up the algorithm that is being proposed. The timing offset estimation presents an element of ambiguity in the use of the conventional correlation scheme for accurate symbol timing detection. However, the use of the preamble conjugate symmetric characteristic that has been proposed in this paper, presents a clear view at the correct timing. Moreover, it is also able to continuously control the position of the FFT window with the first order loop filter. In the end, the results of the simulation clearly showcase that the proposed algorithm gains superiority in comparison to the conventional one.

KEYWORDS : Wireless MAN, OFDM, Synchronization of Timing for FFT, Frame Synchronization

The adoption of OFDM in the fields of wireless Local Area Network (LAN) systems is mainly due to its elevated spectral robustness and efficiency to the multi path fading (Mostofi and Cox, 2006). Due to this, it has also received considerable amount of attention in the wireless Mobile Area Network (MAN) systems, in recent times, under the mobile channel environment (Mostofi and Cox, 2006). The frame synchronization in the burst mode wireless Mobile Area Network is supposed to identify the righteous symbol timing for OFDM quick and in an accurate manner, for the demodulation of data symbols that are transmitted on a continuous basis, following preamble symbol (Mostofi and Cox, 2006). Moreover, tracking timing offset for FFT is needed within the frames data region, as the CIR (Channel Impulse Response) might show rapid changes in the multipath Rayleigh fading channel have elevated mobility (Mostofi and Cox, 2006).

The main reason for the popularity of OFDM technique is due to its ability to provide higher bit rates in wireless communications. Moreover, higher spectral efficiency, along with, immunity related to efficient multipath are 2 of the key elements present in it (Mostofi and Cox, 2006). However, systems for OFDM are also more vulnerable to making mistakes in synchronization, in contrast to the single carrier systems (NI Developer Zone, 2012). This is specifically the case in errors related to frequency of carrier and the timing of symbol (Mostofi and Cox, 2006).

The estimation of symbol time (ST) becomes crucial in the entire process of OFDM synchronization (Mostofi and Cox, 2006). This is because it gives an estimation of the symbol boundary for the remainder of the process involved in synchronization (NI Developer Zone, 2012). An OFDM receiver needs to synchronize with the path that arrives first, to take complete advantage of the interval for guard (Mostofi and Cox, 2006). On the other hand, a bad estimation of the symbol time (ST) will result in severe degradation in performance, such as the loss in signal-to-interference-and-noise ratio (SINR) introduced by inter symbol interference (ISI) (Mostofi and Cox, 2006).

The proposed algorithm is distributed into 2 different parts: Synchronization of frame and synchronization of timing for FFT (Yang et al., 2006). Synchronization of the frame utilizes the characteristics of conjugate-symmetric in order to overhaul the element of ambiguity that is evident in the conventional correlation scheme (Yang, et al., 2006). On the other hand, synchronization of timing for FFT that uses shift in correlation buffer and the system of tracking the estimated timing offset is differentiated from the synchronization based on conventional scheme (Yang, et al., 2006).

Following will be discussed in this paper. The structure for signal and systems have been introduced in the next section, followed by the method of timing synchronization for frame and FFT in the section for Materials and Methods. Moreover, the section next to it

[1]**Corresponding author**

presents the performance results for the algorithm that has been proposed and finally, section 6 would present conclusions on the overall paper.

SYSTEM MODEL

Figures, 1 and 2 represent the burst frame format structures that is being used in this paper, along with a block diagram for the algorithm of OFDM timing synchronization that has been proposed (Wang et al., 2006). Figure 1 shows the insertion of preamble symbol before the data symbol transmission, having roughly three repetition times by assigning pilots through the intervals of three subcarriers (Wang et al., 2006). The transmission of preamble symbol pilots shall take place with the modulation of BPSK (Cheng, 2006). Figure 2 portrays the structure that has been proposed that is comprised of a part from the synchronization of frame (dotted line), as well as, from the synchronization of the timing for FFT (chain line) (Wang et al., 2006).

The sample of n-th OFDM rn of the signal received r(t) that has been corrupted by the fading multipath and includes the offset of frequency Δf is shown through the following equation (Rohling, 2011).

$$r_n = \left\{ \sum_{i=0}^{I-1} \rho_{i,n} e^{j\theta_{i,n}} s_{n+\tau_i} \right\} \cdot e^{j(2\pi\Delta f \cdot nT_s + \theta_0)} \quad (1)$$

where I represents the amount of path delayed, also including signal received and ρi,n, τi, θi,n are time delay, amplitude and phase of the reflected signal of i-th, respectively (Wang et al., 2006). Θo represents a constant phase, whereas, Ts represents the interval for sampling and sn portray the transmitted sample in the domain of the time .

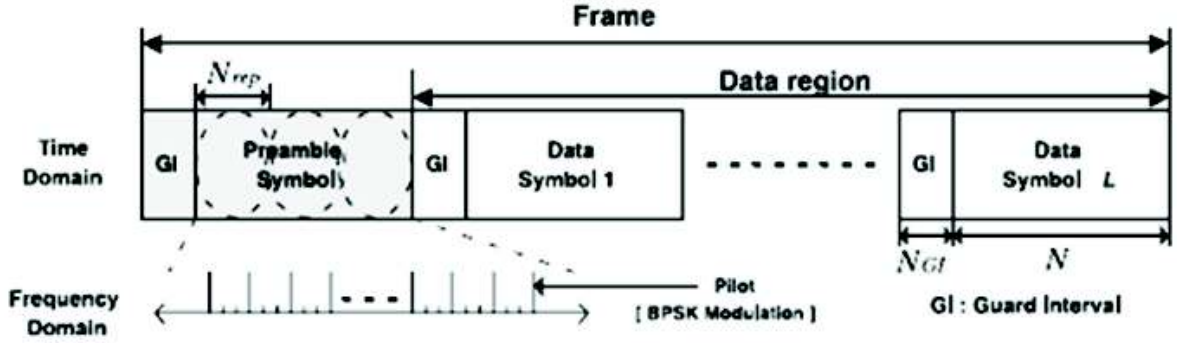

Figure 1 : Frame Format Structure

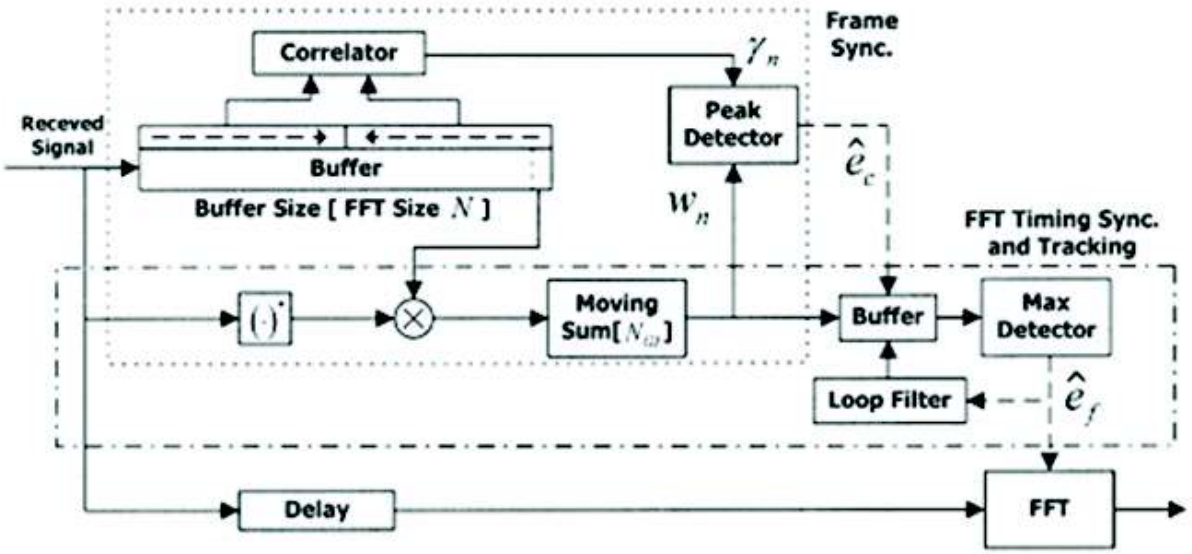

Figure 2 : Proposed Timing Synchronization Block Structure

MATERIALS AND METHODS

Synchronization of Frame

Conventional Method

The delay in correlation among $r_{n+2Nrep+1}$ and rn by samples of $(2N_{rep}+ 1)$ is shown through the following equation:

$$P_n = \left| \sum_{l=0}^{N_{rep}-1} r_{n+l} r^*_{n+l+2N_{rep}+1} \right| \quad (2)$$

The moving average for the period of interval for guard is used to eradicate the plateau for timing metrics in Equation (3) (Chiueh and Lai, 2012). Moreover, the determination of the maximum value for Mn can lead towards the detection of the frame time.

$$M_n = \frac{1}{N_{Gl}} \sum_{m=0}^{N_{Gl}-1} P_n \quad (3)$$

$$\hat{e}_c = \underset{n}{Max} \left[M_n \right] \quad (4)$$

Proposed Method

Sn represent the signal for time domain that is transformed through the symbol ak with the modulation of BPSK in the frequency domain (Tang and Leus, 2007). The association among the signal of time domain Sm at the sample m-th and SN-m at the sample (N-m)-th is based on the fact that they represents each other's complex conjugate, as is also shown in both, Equation (5) and Equation (6) (Chiueh and Lai, 2012).

$$s_{N-m} = \sum_{k=0}^{N-1} \alpha_k e^{j 2\pi \frac{k}{N}(N-m)} = \sum_{k=0}^{N-1} \alpha_k e^{-j 2\pi \frac{k}{N} m}$$

$$= \left(\sum_{k=0}^{N-1} \alpha_k e^{j 2\pi \frac{k}{N} m} \right)^* = s^*_m \quad (5)$$

$$s_n = s^*_{N-n} \quad (6)$$

The execution of the proposed method is carried out through the addition of the values of the product among 2 samples that have the features of Equation (6) (Tang and Leus, 2007). ˆec is the offset for frame timing, the estimation of which is done by finding the position of sample n of the maximum peak value at the output of the Equation (7) (Chiueh and Lai, 2012).

$$\gamma_n = \left| \sum_{l=1}^{(N/2)-1} r_{n+l} \cdot r_{n+N-l} \right| \quad (7)$$

$$\hat{e}_c = \underset{n}{Max} \left[\quad_n \right] \quad (8)$$

r_n was derived through the computation of Equation (1) and is written again in the following equation, with signal for path comprising of the greatest amplitude pm and other reflected paths signal U_m.

$$r_n = \left\{ \rho_{m,n} e^{j\theta_{m,n}} s_{n+\tau_m} + U_n \right\} \cdot e^{j(2\pi\Delta f \cdot nT_s + \theta_0)} \quad (9)$$

$$U_n = \sum_{i=0, i\neq m}^{l-1} \rho_{i,n} e^{j\theta_{i,n}} s_{n+\tau_i} \quad (10)$$

Through the use of Equation (9) and (10), expression of equation (7) can be done in the following manner:

$$\gamma_n = \left| \sum_{l=1}^{(N/2)-1} \left\{ \rho_{m,n+l} e^{j\theta_{m,n}} s_{n+l+\tau_m} + U_{n+1} \right\} \right.$$

$$\cdot \left\{ \rho_{m,N-n+l} e^{j\theta_{m,N-n}} s_{n+N-l+\tau_m} + U_{n+N-l} \right\}$$

$$\left. e^{j(2\pi\Delta f \cdot (2n+N)T_s + 2\theta_0)} \right| \quad (11)$$

$$= \left| \sum_{l=1}^{(N/2)-1} \left\{ h_{m,n} \cdot h'_{m,n} \cdot s_{n+l+\tau_m} \cdot s_{n+N-l+\tau_m} \right.\right.$$

$$+ h'_{m,n} \cdot s_{n+N-l+\tau_m} \cdot U_{n+l}$$

$$\left.\left. + h_{m,n} \cdot s_{n+l+\tau_m} \cdot U_{n+N-l} + U_{n+l} \cdot U_{n+N-l} \right\} \right|$$

$$\approx \left| h_{m,n} \cdot h'_{m,n} \cdot \left| s_{n+l+\tau_m} \right|^2 \right| \quad (12)$$

where, $p_{m,N-n+l}e^{j\theta m-N-n}$ and $p_{m,n+l}e^{j\theta m,n}$ have been replaced with $hl_{m,n}$ and $h_{m,n}$.

Equation (11) shows that the rotation phase of $2\pi\Delta f \cdot nTs + \theta o$ in Equation (9) is transformed into the offset of constant phase $2\pi\Delta f \cdot (2n + N) Ts + 2\theta o$. Therefore, the method that has been proposed becomes independent from the offset of carrier frequency (Tang and Leus, 2007). The

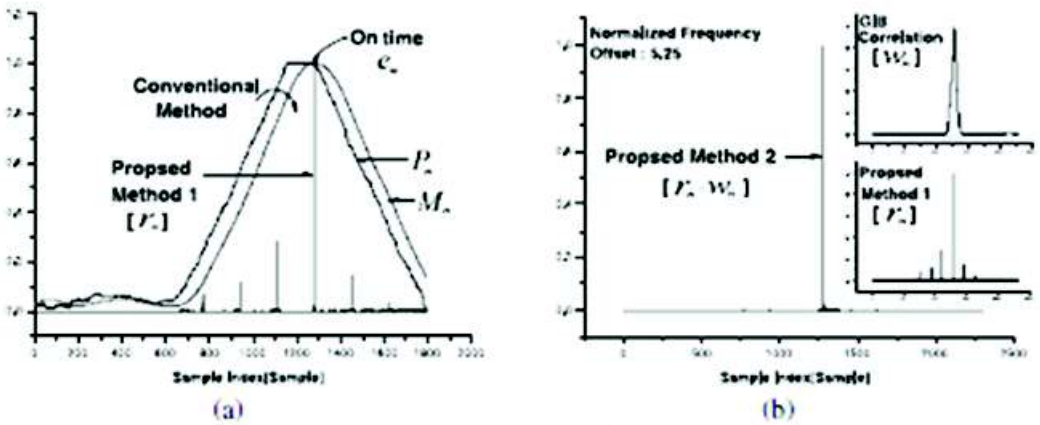

Figure 3 : Frame Synchronization Output

expansion of Equation (12) employs the fact that the signal of OFDM in the time domain can be measured by the Gaussian random variables that have been distributed independent identically, with unit variance and zero mean . However, the yn output highlights a number of different values at the peak as is portrayed in Figure 3(a)-(Method 1) that owes to the similar patterns; the repetitive pattern of the symbol for OFDM by rule of pilot subcarrier allocation and the corresponding of interval for guard to the end of the useful part of symbol (Keller and Mandarini, 2001).

Over the mobile channel environments, there is a possibility for the detection of error related to other peak value because of the effect of the two varying values of channel, hm.hlm in Equation (12) (Keller and Mandarini, 2001). Therefore, the interval for guard correlation output in Equation (13) is additionally exploited by us that relies on

$$w_n = \left| \sum_{l=0}^{N_{GI}-1} r_{n+l}^{*} \cdot r_{n+N+l} \right| \quad (13)$$

$$\hat{e}_c = \underset{n}{Max} \left[\gamma_n \cdot w_n \right] \quad (14)$$

$$\hat{e}_c = \underset{n}{Max} \left[\gamma_n \right], \begin{cases} \bar{e}_c - N_{GI} < n < \bar{e}_c + N_{GI} \\ \bar{e}_c = Max \left[w_n \right] \end{cases} \quad (15)$$

the timing synchronization of the FFT window (Keller and Mandarini, 2001). As only the righteous peak value of timing is found during the process of the GIB with value of correlation that shows both, a gradual increase and a gradual decrease, frame timing estimation is realized through the product of wn and yn as in Equation (14), the output of which has been portrayed in Method 2 in Figure (3)b (Djurisic and Prasad, 2012). In order to decrease product operation complexity, the scheme of comparison between the maximum value of yn and the range of wn, as shown in Equation (15) can be adopted (Zhou, 2005).

Synchronization of Timing For FFT

The proposed method for the synchronization of timing for FFT is shown in Figure 4 that puts the output obtained through GIB correlation at an average and makes estimation for the offset of the timing for FFT (Keller and Mandarini, 2001). This estimation is made by measuring the difference among the maximum value position and the

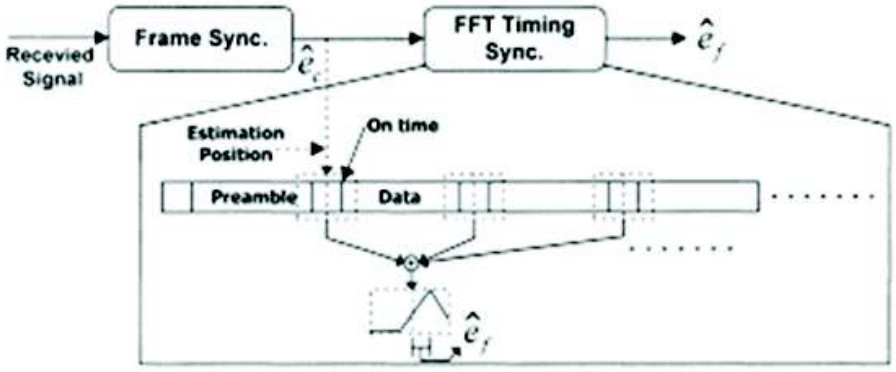

Figure 4. Method for the Synchronization of Timing for FFT

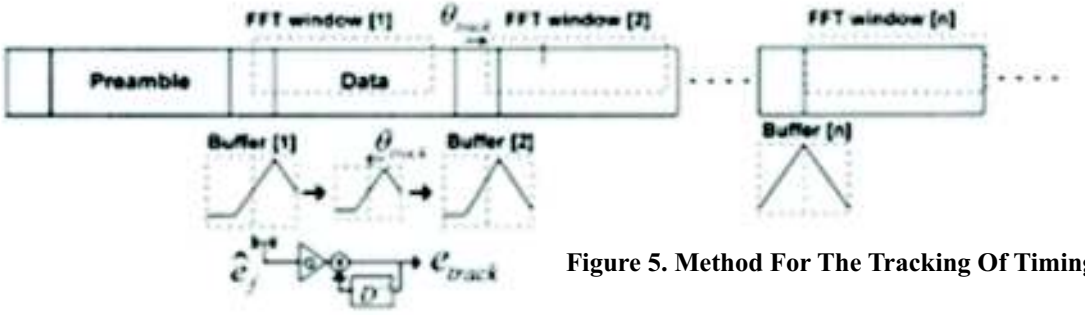

Figure 5. Method For The Tracking Of Timing For Fft

middle value position in the buffer (Cheng, 2006). With averaging, the estimation for the offset of the timing for FFT would be more accurate on a channel for multipath fading, as there is an increase in the number of OFDM symbols received (Cheng, 2006). The range of the maximum sample offset, the estimation of which can be made through the synchronization of the frame is used in order to measure the size of the buffer (Cheng, 2006). Figure 5 shows that tracking for the offset of timing for FFT is done by the 1-st order loop filter that reins estimation for the offset of timing for FFT ˆef with the loop filter gain G and by shifting the correlation value in the buffer (Djurisic and Prasad, 2012).

Equation (13) is written again as Equation (16) with the initial correlational sample (λ), along with, index for the OFDM symbol (s) (Raghavendra , 2005). Moreover, output for the loop filter ($\hat{e}_{track,s}$) is presented in Equation (18).

$$C_{s,\lambda} = \left| \sum_{l=0}^{N_{GI}-1} r^{*}_{\lambda-1} \cdot r_{\lambda+N+l} \right| \tag{16}$$

$$\hat{e}_{track,s-1} - \theta_{buf} < \lambda < \hat{e}_{track,s-1} + \theta_{buf}, \tag{17}$$

$$\hat{e}_{track,0>s} = \hat{e}_{e}$$

$$\hat{e}_{track,s} = \sum_{l=0}^{s} G^{l} \cdot \hat{e}_{f,l}, \hat{e}_{f,0} = 0 \tag{18}$$

where θbu f is half of the size of the buffer, and ˆetrack,s−1 is the tracked offset for timing for FFT during the previous index s-1 for symbol of OFDM. Bs,λ expresses the averaging value for correlation of GIB in terms of mode for tracking, which comprises of the current output of correlation for GIB and the shifted output for θ_{track} samples of previous B_s (Raghavendra, 2005). Moreover, the estimation of offset for timing for FFT is shown in Equation (20).

$$B_{s,\lambda} = \frac{s-1}{s} \cdot B_{s-1,\lambda+\theta_{track}} + \frac{1}{s} \cdot C_{s,\lambda},$$

$$\theta_{track} = \hat{e}_{track,s-2} - \hat{e}_{track,s-1} \tag{19}$$

$$\hat{e}_{fs,} = \underset{\lambda}{Max} \left[B_{s,\lambda} \right] - \theta_{Mid} \tag{20}$$

RESULTS AND DISCUSSION

Results for Simulation

This section provides performance based findings for the simulation of the method that has been proposed for the synchronization of timing in the Additive White Gaussian Noise (AWGN) and multipath Rayleigh fading channels based on vehicular-A of the ITU channel model.

Table 1 :Parameters for Simulation

Parameters	Value
Frequency of Carrier (F_c)	2.3 GHz
Bandwidth (BW)	10 MHz
Spacing of Sub-carrier (┌F)	9.765 KHz
Size of FFT (N)	1024
Interval for Guard (T_g)	12.8 µs (= T_b/8)
Duration for Symbol (T_b)	102.4 µs
# of Data symbols	26 symbols

The highest observed frequencies for Doppler are 6.389 Hz, 127.77 Hz, 255.556 Hz and 425.926 Hz. Table 1 presents a summary of the major parameters of simulation. SNR relies on two elements in this paper, i.e., the ration for the power of noise and the power of signal for data symbol (Zhou, 2005). The offset for frequency that has been normalized by a subcarrier interval is supposed to be 5.25. Moreover, the

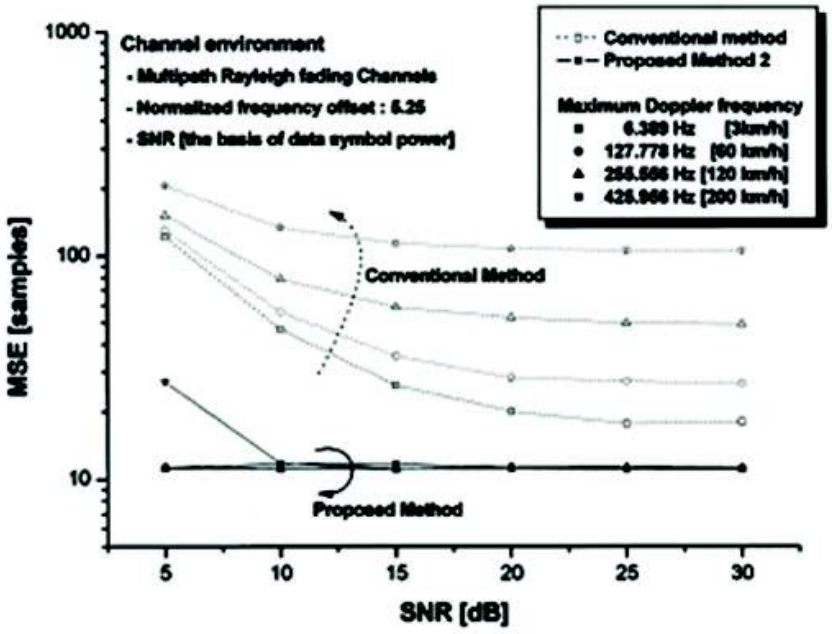

Figure 6 : MSE Performance For The Synchronization of Frame

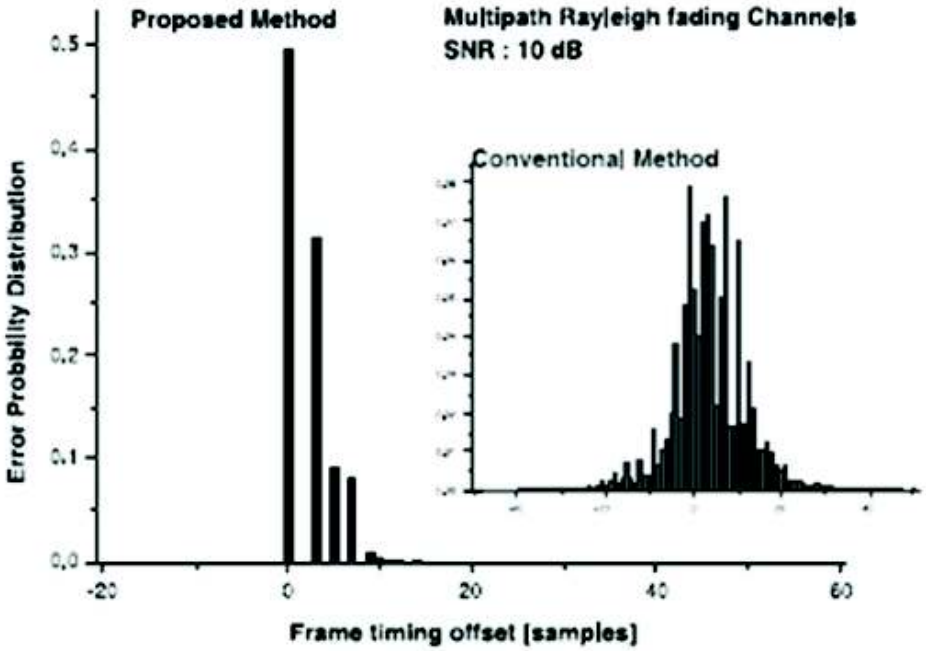

Figure 7: Distribution of Probability for Error in Timing

loop gain for time tracking of FFT window is found to be 0.5.

Figure 6 portrays the fact that the method that has been proposed for the timing of frame in multi-path channel possesses lesser MSE, when compared with that to the conventional method. Moreover, it also highlights the fact that there is not much difference in the performance, which is quite identical, irrespective of the speediness of the mobile (Lv and Chen, 2005). The AWGN channel performances are eliminated, as the method that has been proposed is accurately able to detect timing of the frame over the SNR 0 dB (Zhou, 2005). Furthermore, the error for timing histogram following the process of synchronization of frame in the channel for multi-path Rayleigh fading has

been showcased in Figure 7. The value for ee = ˆec - eo is presented on the horizontal axis in figure 7. It is quite evident through these results that the higher MSE (around 11 samples) from the method that was proposed is needed, in order to detect the delay path having maximum amount of power that is present in the reflected paths. Apart from this, figure 8 reflects the offset in timing, along with, jitter performance of tracking, through a combination with frame synchronization (Zhou, 2005). There is a presence of two biased performances in multi-path for the channel model that has been adopted and having biased values that get lower with an increase in the velocity (Lv and Chen,2005). In Figure 8(a and b), the offset in timing at the start is around 2.5 samples that are associated with the performance of mean in the synchronization for frame.

CONCLUSION

The focus of this paper was to present a synchronization based algorithm for detection of the timing for burst frame, along with the tracking of timing for FFT window. Moreover, it is also found that the algorithm that was proposed turns out to be appropriate for the initial, as well as, for the fine synchronization of timing (Djurisic and Prasad , 2012). Furthermore, this algorithm also possesses the advantage of being able to detect the offset for timing, without the recognition of any information related to pilot. The results of the simulation highlight the fact that the algorithm proposed gives a better performance in comparison to the conventional method in detecting the timing for burst frame. Furthermore, the performance of jitter also improves with an increase in the index for symbol of the OFDM.

REFERENCES

Cheng C., 2006.Maximum-likelihood estimation of frequency and time offsets in OFDM systems with multiple sets of identical data.IEEE Trans. Signal Process, **54**(7): 2848-2852.

Chiueh T. and Lai, 2012.Baseband Receiver Design for Wireless MIMO-OFDM Communications.John Wiley & Sons:115-120.

Djurisic K. and Prasad, 2012.OFDM Based Relay Systems for Future Wireless Communications.River Publishers:95-103.

Keller P. and Mandarini H. ,2001.Orthogonal frequency division multiplex synchronization techniques for

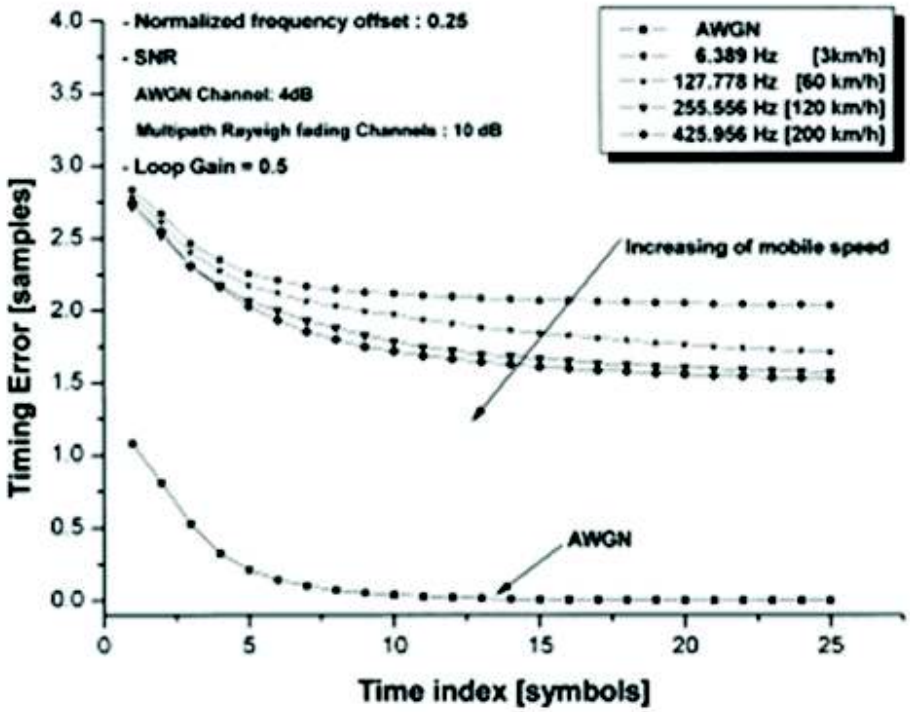

(a) Performance of Timing Error

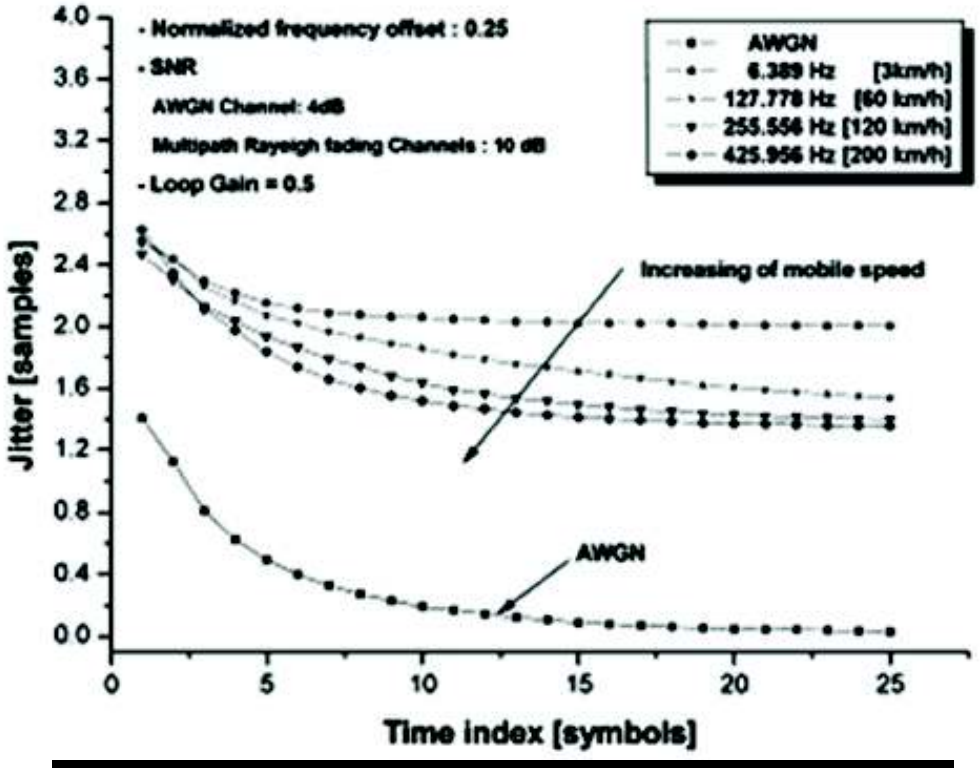

(b) Performance of Jitter

Figure 8 (a and b) : Tracking Performance

frequency selective fading channels. IEEE J. Selected Areas in Communications, **19**(6)999-1008.

Lv Li and Chen 2005.Joint estimation of symbol timing and carrier frequency offset of OFDM signals over fast time-varying multipath channels.IEEE Trans. Signal Process, **53**(12):4526-4535.

Mostofi and Cox, 2006. Mathematical analysis of the impact of timing synchronization errors on the performance of an OFDM system. IEEE Trans. Commun., **54**(2) 226-230.

NI Developer Zone, 2012.Timing and Synchronization in NI LabVIEW, National Instruments. Retrieved from: http://www.ni.com/white-paper/11466/en.

Raghavendra G. 2005.Improving channel estimation in OFDM Systems for sparse multipath channels.IEEE Signal Processing Letters, **12**(1):5255.

Rohling, H., 2011.OFDM.Springer:81-89.

Tang C. and Leus, B. ,2007. Pilot-Assisted Time-Varying Channel Estimation for OFDM Systems. IEEE Transactions on Signal Processing, **55**(5):2226-2238.

Wang S. ,Wang P. andYang Y.,2006. A general SFN structure with transmit diversity for TDS-OFDM system. IEEE Trans. Broadcasting,52 (2):245-251.

Yang Ai , Pan, Ge and Wang Lu,2006.On the synchronization techniques for wireless OFDM systems. IEEE Trans. Broadcasting, **52** (2):236-244.

Zhou H. ,2005.A maximum likelihood fine timing estimation for wireless OFDM systems in Proc. 2005 IEEE 6th workshop on Signal Processing Advances in Wireless Communications:705-709.